

METHOD TO REDUCE FORCE AND TARGET MOVEMENT DURING SURGICAL NEEDLE INTERVENTIONS

T.K. Podder¹, J. Sherman¹, D.P. Clark^{1,5}, D. Fuller¹, D.J. Rubens^{2,4,5},
E.M. Messing^{3,4}, J.G. Strang², L. Liao^{1,2}, W.S. Ng⁶, and Y. Yu^{1,5}

Departments of ¹Radiation Oncology, ²Radiology, ³Urology, and ⁴Surgery
University of Rochester Medical Center, Rochester, NY 14642, USA.

⁵Department of Biomedical Engineering,
University of Rochester, Rochester, NY 14642, USA.

⁶Department of Mechanical and Aerospace Engineering,
Nanyang Technological University, Singapore 639798.

tarun_podder@urmc.rochester.edu

Abstract: During needle insertion in soft tissue or material three forces, namely stiffness force, friction force and cutting force are experienced. Of these forces, friction force contributes the major portion. Thus a higher friction force is partly responsible for larger deformation and movement of soft tissues and organs during numerous medical diagnostic and therapeutic procedures. In this study we investigate the effectiveness of needle coating to reduce friction force, and thereby tissue deformation or movement during surgical procedures. From experimental results we observe that various coatings, especially carbon and Teflon coating, reduce needle intervention forces, which in turn decrease target movement significantly.

Introduction

Accurate percutaneous intervention and precise placement of surgical needles are very important in various medical diagnostic and therapeutic procedures like biopsy, cryo-ablation, laser-ablation, brachytherapy, thermo-ablation, etc. Utilizing computer assisted imaging techniques and robotic systems, several researchers have attempted to reach a desired target in soft tissue assuming known target position in 3D, no target movement, and a straight needle path [1-7]. These assumptions are difficult to realize in practice because of several reasons such as tissue heterogeneity and elastic stiffness, tissue deformation and movement, unfavorable anatomic structures, needle bending, inadequate sensing, and poor maneuverability. Some of the factors such as needle bending, tissue deformation and movement are directly proportional to forces and torques experienced by the needle during interstitial intervention. Thus, reduction of force on the needle can reduce the target movement and enhance

surgical interventions. Therefore, understanding of the complex mechanism of needle interaction with soft tissue is an area of active research. Several research groups have been working on needle force measurement, modeling of soft tissue and its interaction with needle [1-17]. Most of the researchers agree that a complete model of the force experienced during needle insertion into soft tissues require a combination of empirical and analytical modeling. They have emphasized thorough testing and in-depth analysis, development of new testing and modeling methodologies, and multiple model (e.g. deformation, friction, and optimal speed) integration for better understanding and re-generating the complex *in vivo* soft tissue environment during various percutaneous interventions [8-17]. Target movement due to organ deformation is critical in percutaneous procedures because it may create complications such as vital tissue damage, misdiagnosis, under/over dosing with radiation, tumor seeding, etc. During prostate brachytherapy, clinicians have observed about 5-15mm movement of the prostate when the needle hits the capsule [18]. Reported work on the study of needle properties and velocity modulations in an attempt to reduce target movement is limited.

In the present work we have investigated the effects of insertion velocity on target movement and needle coatings on forces experience by the needle. Reduction of force on a needle can be an alternative method, as opposed to organ arrest or immobilization using other techniques to reduce target deflection during needle insertion in soft tissues. In this paper, we present the efficacy of needle coatings and insertion velocity modulation during surgical needle insertion in soft materials. We have verified our hypotheses of needle insertion force reduction and the target movement

minimization by performing experiments with various insertion speeds of needles having several types of coatings.

Experiment Setup

We have fabricated a 6 DOF (degree-of-freedom) robotic system for needle insertion experiments (Figure 1). All the motions of the robot are actuated by stepper motors. Two linear optical encoders with 10 μ m resolution are mounted on x, and y-axes. A rotary optical encoder with 5 μ m resolution is fitted on z-axis. The rotational positions about x-axis and y-axis are also monitored by optical encoders with 5 μ m resolutions. A 6 DOF force/torque (F/T) sensor, (Nano25[®], ATI), is mounted aligning its z-axis parallel to the robot's z-axis. The robotic system is kinematically controlled; commands are sent using LabVIEW[™] (version 7.1 from National Instruments).

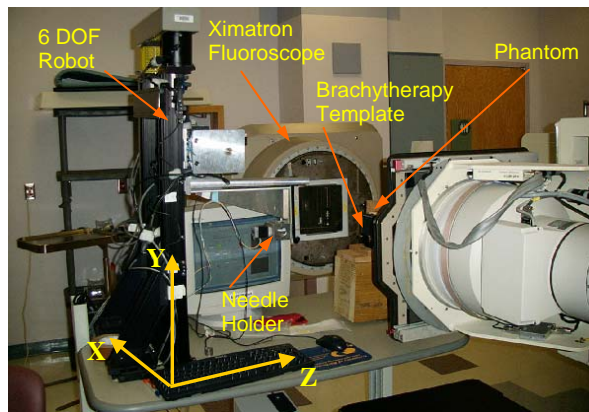


Figure 1(a): Test setup a 6 DOF robotic test-bed with fluoroscopy machine.

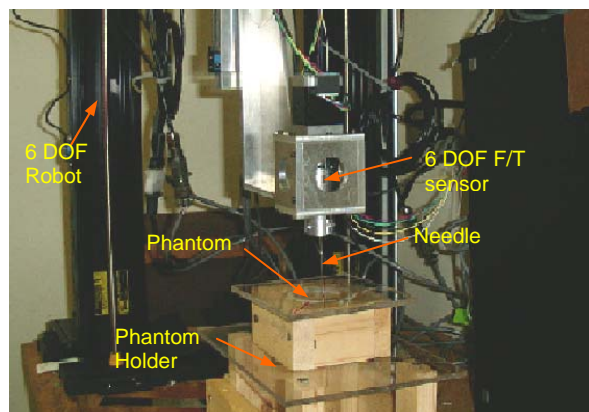


Figure 1(b): The 6 DOF robotic test-bed equipped with a 6 DOF force/torque sensor.

The software is executed on Windows XP in a Pentium[®] 4, 1.6GHz computer with graphical user interface (GUI), which we developed. The fluoroscope used for measuring the target movement is the Ximatron[®] C-series

Radiotherapy Simulator, (manufactured by Varian Oncology Systems) having a maximum field size of 40cm x 40cm. The voltage and current settings for image acquisition during our experiment were 75kV at 4mA, respectively. Normal settings during actual patient film acquisition range from 60kV–129kV at 200mA, with a rate range of 20mAs–200mAs.

Methods and Materials

Three types of 18-gauge (18G, i.e. 1.27mm in diameter) brachytherapy needles were used; two of them were coated with Teflon and carbon, the third one was commonly used commercial brachytherapy needle whose coating was unknown. Needles were inserted by the 6 DOF robotic system (shown in Figure 1) in soft material phantoms prepared from polyvinylchloride (a super soft plastic, commonly known as PVC supplied by MF Manufacturer, TX) mixing with 25% softener. Maximum force and torque measurement capacities of the Nano25[®] F/T sensor that is mounted on the end effector of the robot are: $F_x=125N$, $F_y=125N$, $F_z=500N$, $T_x=3N.m$, $T_y=3N.m$, and $T_z=3N.m$; sensor resolution was of the order of 10^{-3} . Force-torque data were collected at 100Hz using a Pentium 4 PC equipped with LabVIEW 7.0 software.

We performed experiments with insertion/linear velocities at 5mm/s, 10mm/s, 25mm/s 50mm/s and 200mm/s. The force/torque data were acquired using the 6 DOF F/T sensor; the needle travel distance was measured using motor encoders. We have used fluoroscopy (X-ray) to assess the target deflection in phantom at different speeds of needle insertion. The PVC phantoms used with three different dimensions were: (i) cylindrical phantom with 5.08cm in diameter and 5.08cm in length (Figure 1(b)), both ends open; needles penetrated through the phantom and moved beyond the phantom; (ii) cylindrical phantom with 7.5cm in diameter and 15.5cm in length, both ends open; needles penetrated about 12cm into the phantoms (Figure 1(a)); and (iii) box phantom with 4.0cm width, 5.0cm depth and 10.cm height, two 2cm diameter holes were provided on both sides of 4.0cm dimensions for needle entry.

To assess the friction force alone, the needle tips were passed through the phantom; only the cannulas were in contact with the material. For evaluating target movement using fluoroscopy, two small pieces of a highly flexible radio-opaque wire of 0.2mm diameter were placed approximately at 1.5cm and 6.5cm in each of the phantoms (prior to solidification of PVC). We measured the movements of the target wires relative to the cross-wire of the fluoroscopy and the reference wires fixed outside the phantom cylinder. All data were averaged from 5 insertions at each velocity of any needle. Force-torque data were smoothed using a 50-point moving average.

Results and Discussions

We have performed extensive experiments to evaluate the effects of needle insertion speed and coating on surgical needle intervention in soft material phantom. Two sets of experiments: (1) *effects of insertion velocity on needle force and target movement*, and (2) *effects of needle coatings* are presented in this section.

Experiment 1: Effects of insertion velocity on needle force and target movement

In this experiment we investigate how the needle force, and target movement vary when the insertion/ linear speeds of the needle are changed. The main portion of the needle motion, i.e. the cruising velocity, was 5mm/s, 10mm/s, 25mm/s, 50 mm/s, 100mm/s, and 200mm/s with both the acceleration and deceleration at 508mm/s². We have selected to perform the experiments at these relatively high velocities because we observed that in many occasions, especially prostate brachytherapy procedures where the surgeons insert the needles at a speed of 200mm/s or higher. The velocity profiles for insertion as well as retraction were identically trapezoidal with 508mm/s² acceleration and deceleration.

The results from the experiments are presented in Figures 2 & 3 (forces on Teflon coated needle), Figure 4 (forces on commercial needle), and Figures 5 & 6 (target deflections).

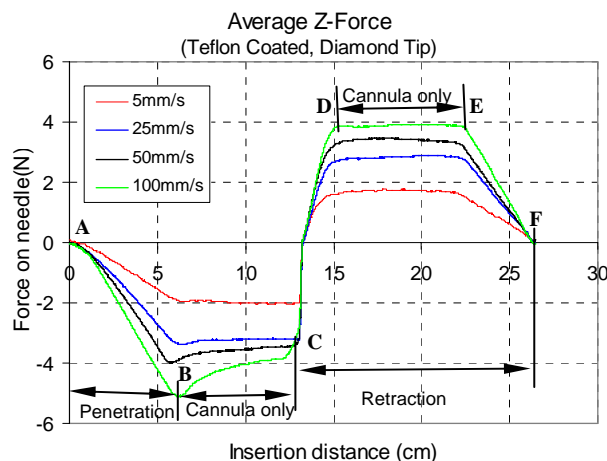


Figure 2: F_z force on diamond tip Teflon coated 18G needle at different insertion velocities. The cylindrical PVC phantom was 5.08cm in diameter and 5.08cm in length with both ends open; the needle went through the phantom and traveled further up to a total of 13.5cm, then retracted to the starting point.

From plots in Figures 2 & 4, it is observed that the main insertion force, i.e. z-force (F_z) increases with increasing insertion/ linear velocity. For the Teflon coated needle (Figure 2) we have increased the insertion in the

ratio of 5, 2 & 2 speeds (5mm/s, 25mm/s, 50mm/s, & 100mm/s); however the changes in force at the end of penetration, i.e. near point “B” appear to be in a different ratio, i.e. 1.7, 1.2 & 1.3.

For the commercial needle (Figure 4), insertion speeds were varied in the ratio of 2, 2.5, 2, 2 & 2 (5mm/s, 10mm/s, 50mm/s, 100mm/s & 200mm/s); but the changes in force at the end of penetration, i.e. the “10cm” point appear to be in a different ratio, i.e. 1.8, 1.3, 1.1, 1.2, & 1.1. The maximum change in insertion speed occurred between 5mm/s and 10mm/s. This behavior can be attributed to the non-linear nature of soft material, i.e. the PVC, which has a strain rate related complex elastic modulus.

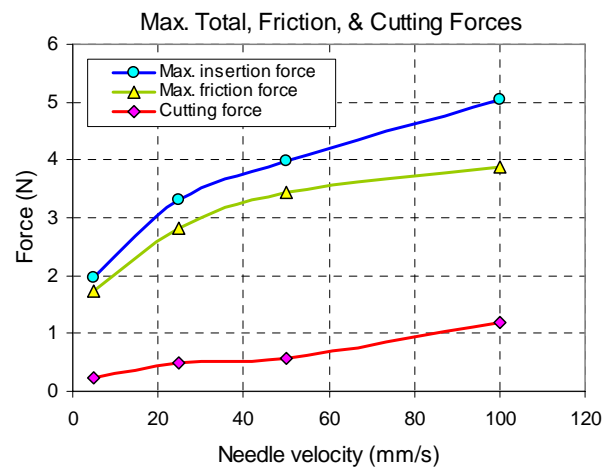


Figure 3: Maximum total penetration force, friction force and cutting force while Teflon coated 18G diamond tip needle is inserted into PVC phantom.

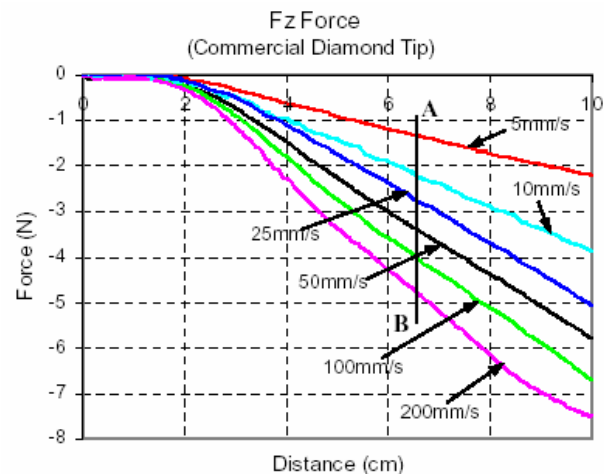


Figure 4: F_z (main penetration) force on diamond tip commercial 18G needle at different insertion velocities. The cylindrical PVC phantom was 7.5cm in diameter and 15.5cm in length with both ends open; the needle was penetrated about 12.0cm into the phantom.

In Figure 2, part “A-B” corresponds to needle insertion. The force is increasing due to a combination of

the cutting force and the increasing frictional force as more needle is inserted into the phantom; point “B” is the point in which the needle has passed through phantom, i.e. cutting action is over, and the forces reduce. Therefore, from this point (close to “B”) we can estimate the cutting force (which includes elastic stiffness force, cutting force, and friction force). Throughout the “B-C” portion, the cannula of the needle is the only part in contact with the phantom material; therefore we can consider this force the friction force. Just before point “C” the needle stops for 60sec and the phantom gradually relaxes before retracting. Portion “C-D” is a combination of reverse stiffness force and friction force (static, partly dynamic, and viscoelastic) on the needle until point “D”. “D-E” is the cannula touching the phantom material during retraction, and the predominant dynamic friction and viscoelastic forces with flat profiles are observed. After point “E” the length of emersion of the needle in the phantom gradually lessens and thus the force reduces accordingly until the needle is totally out of the phantom at point “F”. If we superimpose part “E-F” on part “A-B” in reverse order, then we can get the cutting forces during insertion which are 0.23N, 0.5N, 0.55N, and 1.18N at 5mm/s, 25mm/s, 50mm/s, and 100mm/s insertion velocities (Figure 3).

results, it is observed that target movement increases with an increase in insertion velocity (ref. Figures 5 & 6). Therefore, from these results we can infer that a decrease in insertion force will in turn reduce the target movement, as shown in Figure 7.

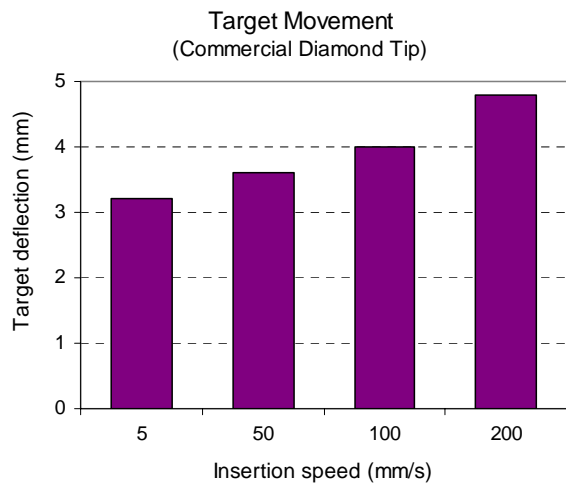


Figure 5: Target deflection/movement in PVC phantom at different insertion speeds (5mm/s, 50mm/s, 100mm/s & 200mm/s) while commercial 18G diamond tip brachytherapy needles were penetrated.

Movement of the target, i.e. the 0.2mm diameter flexible radio-opaque wire embedded in PVC, was observed under fluoroscopy. The target wire was at 6.5cm from the entry point of the needle; the corresponding insertion forces are marked with a vertical line and labeled “A-B” in Figure 4. In Figure 5 we present the target deflection at different insertion speeds; here we observe an increase in deflection with speed. The insertion force, insertion speed and target movement are plotted in Figures 6 & 7 and we observe a strong correlation between all three. From our experimental

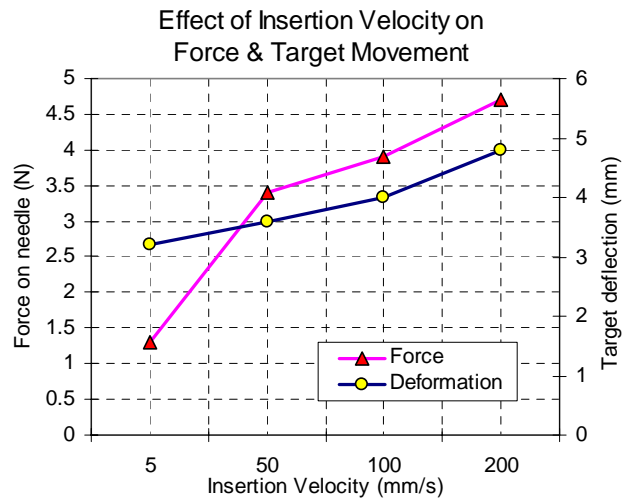


Figure 6: Target deflection/movement in PVC phantom at different insertion forces.

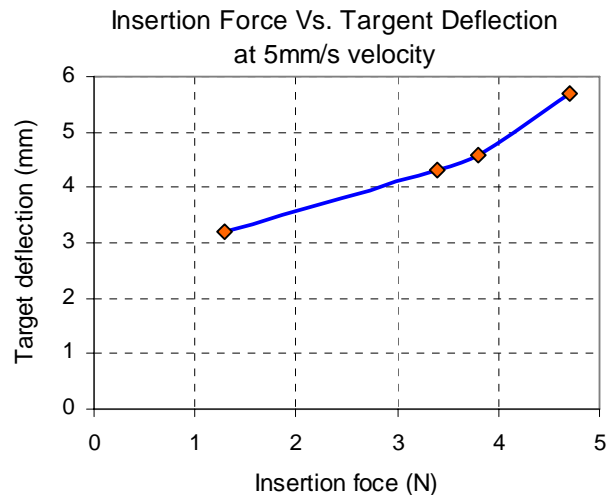


Figure 7: Effect of insertion force on target movement (deflection increases with speed).

Experiment 2: Effects of needle coatings

In this experiment we have used three types of 18-gauge (18G) brachytherapy needles; one of them coated with Teflon (done by Donwell Company, Manchester, CT), the other with Carbon (done by Argonne National Lab., Argonne, IL). We have compared the results of the two coated needles with a commonly used commercial needle whose coating is unknown (Mick Radio-Nuclear

Instruments, Mt. Vernon, NY). The PVC phantom was prepared in a square box with 25.5cm length & width, and 5.0cm in height. The bottom plate of the box contains a total 25 holes each having 2cm diameters at every 2.3cm to allow the needle to penetrate through the phantom and isolate friction. The experimental results have been presented in Figures 8 and Table 1. From Figure 8, we observe that the commercial needle has the highest insertion and frictional force, while the force on carbon coated needle is the least and the force on Teflon coated needle is in between the aforementioned needles. Similar force patterns are observed in both penetration and retrieval of the needle. The force segment in which friction is isolated and only the cannula is interacting with the phantom material (after the needle tip has passed through the phantom) is marked as “B-D” in the Figure 8. During the “B-C” segment, the phantom material relaxes and after that the friction force is almost constant (“C-D”). The plots in this figure reveal the effectiveness of coatings in minimizing friction force. We also observe a significant reduction in insertion force. Although each needle starts with the same force profile, friction plays a more significant role as the needle is inserted farther into the phantom (more cannula-phantom contact) thus, one would expect the profiles to separate as they approach point “B” (as seen below in Figure 8).

velocity; with higher velocity the friction force reduction rate decreases marginally (for Teflon coated needle 15.62% to 14.01%, and for carbon coated needle 34.54% to 34.42%). It appears that by altering the needle coating, the needle insertion force can be reduced and thereby result in reduced target movement during various percutaneous procedures.

Table 1: Reduction in axial force (mainly friction force) during 18-gauge diamond tip brachytherapy needle insertion in PVC phantom with 25% softener.

Needle type	Needle insertion speed	F _z force @ point “D”	Force reduction
Commercial diamond tip needle	5 mm/s	-1.76 N	--
	100 mm/s	-3.33 N	--
Teflon coated diamond tip needle	5 mm/s	-1.49 N	15.62%
	100 mm/s	-2.87 N	14.01%
Carbon coated diamond tip needle	5 mm/s	-1.15N	34.54%
	100 mm/s	-2.19 N	34.42%

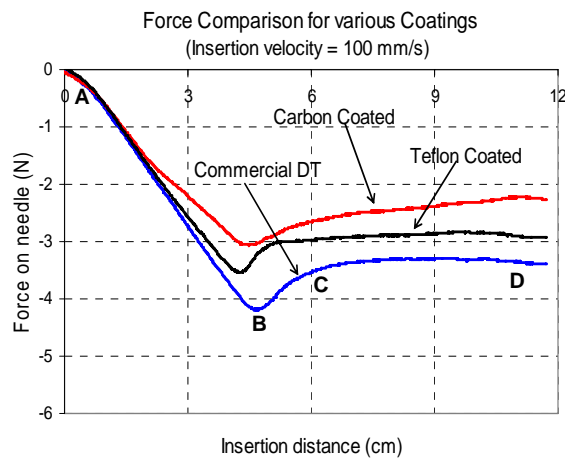


Figure 8: F_z force profile during needle penetration and retrieval in PVC phantom. Two needles were coated with Carbon and Teflon, and the third one was commercial needle.

In Table 1, we present experimental results for three types of needles (commercial, teflon coated, and carbon coated) with two different velocities, i.e. at 5mm/s and 100mm/s. We observe significant reduction in friction force for the Carbon coated needle; the average reduction (in “C-D” portion”) being about 34.5%. Moderate reduction in friction force was noticed for the Teflon coated needle; the average reduction (in “C-D” portion”) is about 15%. It is interesting to notice that there is little effect with change in

Conclusions and Future Work

We have investigated the effects of insertion velocity on target movement in soft material and the efficacy of different coatings on surgical needles in an attempt to reduce insertion force, which is a contributing factor to the target movement during percutaneous interventions. We have used 18G prostate brachytherapy needle and a PVC phantom instead of soft animal tissue. The rationale for choosing homogeneous (or near homogeneous) PVC as our phantom material was due to the heterogenous nature of animal tissues. This would have provided us with inconsistent data and made it difficult to evaluate the effectiveness of the proposed technique.

From the experimental results, we observed a steady increase in main axial force on the needle as the insertion speed increases. With an increase in insertion speed, we noticed a related increase in target movement. Thus, it appears that for precise placement of surgical needle in soft tissue, one must to find the optimal insertion speed to minimize tissue or organ deformation and deflection. We observed a significant advantage to applying frictionless coatings to surgical needles. From our preliminary experimental results (with PVC), it is understood that the carbon coating is the most effective in the reduction of friction force on the needle. Therefore, one of the solutions to reduce tissue and organ deformation and displacement may be the coating of surgical needles with carbon or other ultra-low frictional materials. We will continue our research to evaluate the effects of various coatings on surgical

needles as well as find the optimal speed to minimize target movement.

Acknowledgements

This work is supported by the National Cancer Institute (NCI), under grant number R01 CA091763. The authors would like to thank Mr. Eric Kusmaul for helping in fluoroscopy data collection. The authors would like to extend thanks to Dr. Paul Okunieff and Dr. Michael Schell for providing the facility for fluoroscopy.

References

- [1] LOSER, M., NAVAB, N. (2000): 'A new robotic system for visually controlled percutaneous interventions under CT', Proc. MICCAI (2000) and Lecture Notes in Computer Science, Springer Verlag, **1935**, pp. 887-897.
- [2] STOIANOVICI, D., CADEDDU, J. A., DEMAREE, R. D., BASILE, H. A., TAYLOR, R. H., WHITCOMB, L. L., SHARPE, W. N. JR., KAVOUSSI, L. R. (1997): 'An efficient needle injection technique and radiological guidance method for percutaneous procedures', Lecture Notes in Computer Science, CVRMed-MRCAS, Springer Verlag, **1205**, pp. 295-298.
- [3] PATRICIU, A., MUMITRU, D., PETRISOR, D., KAVOUSSI, L., STOIANOVICI, D. (2003): 'Automatic targeting method and accuracy study in robot assisted needle procedures', Proc. MICCAI (2003) and Lecture Notes in Computer Science, Springer Verlag, pp. 124-131.
- [4] HONG, J., DOHI, T., HASHIZUME, M., KONISHI, K., HATA, N. (2004): 'An ultrasound-driven needle-insertion robot for percutaneous cholecystostomy', J. of Phys. in Med. and Bio., **49**(3), pp. 441-455.
- [5] MAURIN, B., GANGLOFF, J., BAYLE, B., *et al.* (2004): 'A parallel robotic system with Force Sensors for percutaneous procedures under CT-guidance', Proc. MICCAI (2004) and Lecture Notes in Computer Science, Springer Verlag, **3217**, pp. 176-183.
- [6] SCHNEIDER, C.M., OKAMURA, A.M., FICHTINGER, G. (2004): 'A robotic system for transrectal needle insertion into prostate with integrated ultrasound', Proc. IEEE Int. Conf. on Robotics and Automation 2004, New Orleans, USA, pp. 365-370.
- [7] WEI, Z., WAN, G., GARDI, L., DOWNEY, D.B., FENSTER, A. (2004): 'Robotic aided 3D TRUS guided intraoperative prostate brachytherapy', SPIE, **5367**, pp. 361-370.
- [8] O'LEARY, M. D., SIMONE, C., WASHIO, T., YOSHINAKA, K., OKAMURA, A.M. (2003): 'Robotic needle insertion: effect of friction and needle geometry', Proc. IEEE Int. Conf. on Robotics and Automation 2003, pp. 1774-1779.
- [9] KATAOKA, H., WASHIO, T., CHINZEI, K., MIZUHARA, K., SIMONE, C., OKAMURA, A.M. (2002): 'Measurement of the tip and friction force acting on a needle during penetration', Proc. MICCAI (2002) and Lecture Notes in Computer Science, Springer Verlag, **2488**, pp. 271-278.
- [10] MATSUMIYA, K., MOMOI, Y., KOBAYASHI, E., *et al.* (2003): 'Analysis of forces during robotic needle insertion to human vertebra', Proc. MICCAI (2003) and Lecture Notes in Computer Science, Springer Verlag, **2878**, pp. 271-278.
- [11] OKAMURA, A.M., SIMONE, C., O'LEARY, M.D. (2004): 'Force modeling for needle insertion into soft tissue', IEEE Trans. on Biomed. Engineering, **51**(10), pp. 1707-1716.
- [12] KATAOKA, H., WASHIO, T., AUDETTE, M., DIMAIO, S.P. (2001): 'A model for relations between needle deflection, force, and thickness on needle penetration', Proc. MICCAI (2001) and Lecture Notes in Computer Science, Springer Verlag, **2208**, pp. 966-974.
- [13] DIMAIO S.P., SALCUDEAN S.E. (2003): 'Needle insertion modeling and simulation', IEEE Trans. on Robotics and Automation, **19**(5), pp. 864-875.
- [14] ALTEROVITZ, R., POULIOT, J., TASCHEREAU, R., HSU, I.C.J., GOLDBERG, K. (2003): 'Simulating needle insertion and radioactive seed implantation for prostate brachytherapy', Medicine Meets Virtual Reality, edited by J.D. Westwood, IOS Press, **11**, pp. 19-25.
- [15] GEROVICHEV, O., MARAYONG, P., OKAMURA, A.M. (2002): 'The effect of visual and haptic feedback on manual and teleoperated needle insertion', Proc. MICCAI (2002) and Lecture Notes in Computer Science, Springer Verlag, **2488**, pp. 147-154.
- [16] KIMURA, A., CAMP, J., ROBB, R., DAVIS, B. (2002): 'A prostate brachytherapy training rehearsal system – simulation of deformable needle insertion', Proc. MICCAI (2002) and Lecture Notes in Computer Science, Springer Verlag, **2488**, pp. 264-271.
- [17] ALTEROVITZ, R., GOLDBERG, K., POULIOT, J., *et al.* (2003): 'Needle insertion and radioactive seed implantation in human tissue: simulation and sensitivity analysis', Proc. IEEE Int. Conf. on Robotics and Automation 2003, pp. 1793-1799.
- [18] CHENG, G., LIU, H., LIAO, L., YU, Y. (2001): 'Dynamic brachytherapy of the prostate under active image guidance', Proc. MICCAI (2001) and Lecture Notes in Computer Science, Springer Verlag, Vol. **2208**, pp. 351-359.